Performance of the DSA's Subcarrier Demodulation Digital Loop

M. K. Simon
A. Mileant
Telecommunication Systems Section

The subcarrier demodulation digital loop is part of the Baseband Assembly. The subcarrier demodulator is a fourth-order Costas-type loop. It corresponds to a "type 2" analog loop in terms of steady state response. In this article, the expected value and the variance of the error signal are determined as functions of the input SNR. A Nyquist sampling rate of the input signal is assumed. From the integro-difference equations a mixed s/z domain block diagram is obtained. From the loop's transfer function a set of gains for the loop filter is obtained. Also, a set of state equations is presented for future reference. Finally, the noise-equivalent bandwidths are calculated for normalized computation times of 0, 0.25 and 0.5.

The subcarrier demodulator analyzed in this article tracks a parabolic phase input with finite steady state error. Since at each update instant the loop gains are adjusted to compensate for the variations in SNR of the input signal, the noise-equivalent bandwidth is maintained constant.

I. Introduction

The subcarrier demodulation digital loop is part of the Baseband Assembly (Ref. 1). The subcarrier is demodulated by a Costas-type fourth-order digital loop. The input to this loop, which comes from the real-time combiner (RTC), consists of a string of unitless numbers whose values are proportional to the signal and noise amplitudes. For analysis purposes, it is convenient to assume that sampling of the input signal occurs at the Nyquist rate. This is justified by the fact that, according to measurements made by Larry Howard (private communication), oversampling does not appear to improve or degrade the SNR of the loop's error signal.

In this article, the topics are subdivided as follows:

(1) Error Signal Statistics

(2) DCO Board Transfer Function

(3) Phase Detector Averages

(4) Closed Loop Transfer Function

(5) Determination of Gains A, B, C, and D

(6) Steady State Error

(7) Derivation of the State and Output Equations

(8) Noise-Equivalent Bandwidth

II. Error Signal Statistics

The input to the subcarrier demodulation loop (Fig. 1) comes from the RTC. This input can be modeled as a string of samples as follows:

$$y_i = s_i + n_i \tag{1}$$

where s_i is a unitless random variable whose value is proportional to the signal amplitude of the i^{th} sample, and n_i is a unitless random variable whose value is proportional to the noise amplitude of the i^{th} sample.

The signal tracked by the loop is a squarewave subcarrier of N_{sc} Nyquist samples per cycle BPSK modulated by binary random data with N_s Nyquist samples per symbol. The mean of the i^{th} sample is given by

$$E\{s_i\} = b_j \sqrt{S} \cos\theta_i \tag{2}$$

where $b_j = \pm 1$ is a random variable equal to the sign of the j^{th} binary data symbol.

The noise is modeled as a random process with zero mean and variance per sample σ_n^2. The instantaneous phase of the input signal is θ_i.

In the tracking mode, the subcarrier digital phase-locked loop produces an estimate of the input phase, θ_i, with an instantaneous error

$$\phi_i = \hat{\theta}_i - \theta_i \tag{3}$$

To proceed with this analysis, it will be convenient to define the normalized phase error

$$u_i = \frac{\phi_i}{\pi/2} \tag{4}$$

with half symbol average

$$u_k = \frac{1}{N_s/2} \sum_{i=1}^{N_s/2} u_i \tag{5}$$

and one update period average (K symbols per update)

$$u_n = \frac{1}{2K} \sum_{k=1}^{2K} u_k$$

$$= \frac{1}{T_L} \int_{t_n - T_c}^{t_n + T_R} u(t)\, dt \tag{6}$$

Here T_L is the update time interval.

Referring to Fig. 1, the expected value of the outputs of the in-phase and quadrature arms will be, respectively (assuming loop operation in the linear region),

$$\bar{x}_{Ii} = b_j K_1 \sqrt{S}(1 - |u_i|) \tag{7}$$

$$\bar{x}_{Qi} = b_j K_2 \sqrt{S} u_i \tag{8}$$

The outputs of the I and Q summers, which add up $N_s/2$ samples, will have means

$$\bar{x}_{Ik} = b_j K_1 \sqrt{S} \frac{N_s}{2} (1 - |u_k|) \tag{9}$$

$$\bar{x}_{Qk} = b_j K_2 \sqrt{S} \frac{N_s}{2} u_k; \quad k = 1, 2, \ldots, 2K \tag{10}$$

and variances due to thermal noise

$$\sigma_{Ik}^2 = K_1^2 \frac{N_s}{2} \sigma_n^2 \tag{11}$$

$$\sigma_{Qk}^2 = K_2^2 \frac{N_s}{2} \sigma_n^2; \quad k = 1, 2, \ldots, 2K \tag{12}$$

Finally, the error signal ϵ_n at the output of the third summer, which adds up $2K$ half-symbol samples, will have mean value

$$\epsilon_n = 2K \bar{x}_I \bar{x}_Q = \frac{K}{2} K_1 K_2 K_3 N_s^2 S(1 - |u_n|) u_n \tag{13}$$

because $b_j^2 = 1$ for all j.

The variance at the input to the third summer will be

$$\sigma_{IQk}^2 = E[(x_{Ik} x_{Qk})^2 - (\bar{x}_{Ik} \bar{x}_{Qk})^2] K_3^2 \tag{14}$$

$$= (\sigma_{Ik}^2\,\sigma_{Qk}^2 + (\bar{x}_{Ik})^2\,\sigma_{Qk}^2 + (\bar{x}_{Qk})^2\,\sigma_{IK}^2)\,K_3^2 \quad (15)$$

The variance of the output of the third summer will be

$$\sigma_\epsilon^2 = \sum_{k=1}^{2K} \sigma_{IQk}^2 \quad (16)$$

$$= \frac{K}{2} K_1^2 K_2^2 K_3^2 N_s^2\,\sigma_n^4 + \frac{K_1^2}{8} K_2^2 K_3^2 SN_s^3\,\sigma_n^2 \left(\sum_{k=1}^{2K} (1 - |u_k|)^2\right) + \frac{K_1^2}{8} K_2^2 K_3^2 SN_s^3\,\sigma_n^2 \left(\sum_{k=1}^{2K} u_k^2\right) \quad (17)$$

Since the assumption of operation in the linear region implies a high loop SNR condition (small values of u_k), then it is convenient to let $u_k = 0$ in (17), which gives the approximation

$$\sigma_\epsilon^2 = \frac{K}{2}K_1^2K_2^2K_3^2N_s^2\,\sigma_n^4 + \frac{K}{4}K_1^2K_2^2K_3^2\,SN_s^3\,\sigma_n^2 = \frac{K}{2}K_1^2K_2^2K_3^2N_s^2\,\sigma_n^4\left[1 + \frac{SN_s}{2\sigma_n^2}\right] \quad (18)$$

Furthermore, for small u_n the normalized loop tracking curve

$$g(u_n) = (1 - |u_n|)\,u_n \quad (19)$$

can be approximated by

$$g(u_n) = u_n \quad (20)$$

whereupon the mean of the error signal at the third summer output, as given by (13), becomes

$$\bar{\epsilon}_n = G'_Q\,u_n \quad (21)$$

with

$$G'_Q \triangleq KK_1K_2K_3N_s^2\,S/2 \quad (22)$$

III. DCO Board Transfer Function

Referring to Fig. 1, the CPU reads the error signal ϵ_n every T_L seconds (i.e., N_sK samples), and at the input of the DCO board produces increments of phase rate according to the following algorithm:

$$\Delta\hat{\dot{\theta}}_n = A\epsilon_n + B\epsilon_{n-1} + C\Delta\hat{\dot{\theta}}_{n-1} + D\Delta\hat{\dot{\theta}}_{n-2} + E\hat{\ddot{\theta}}_n \quad (23)$$

where A, B, C, and D are gains to be determined, and $\hat{\ddot{\theta}}_n$ is the estimate of the phase acceleration and is an external input to the digital loop. In this analysis, it will be assumed that $E = 0$.

Assuming zero initial conditions, Eq. (23) can be expressed in the z-domain as

$$\Delta\hat{\dot{\theta}}(z)\,(1 - Cz^{-1} - Dz^{-2}) = \epsilon(z)\,(A + z^{-1}B) \quad (24)$$

It should be noted that Eq. (24) assumes zero computation time; i.e., as soon as the CPU reads ϵ_{n-1}, it produces $\hat{\dot{\theta}}_n$. The actual delay between reading ϵ_{n-1} and producing $\Delta\hat{\dot{\theta}}_n$ will be accounted for further on in this analysis.

The transfer function $F(z)$ of the blocks designated in our analysis as the "loop filter" is, from Eq. (24),

$$F(z) = \frac{\Delta\hat{\dot{\theta}}(z)}{\epsilon(z)} = \frac{(Az + B)z}{(z^2 - Cz - D)} \quad (25)$$

The phase rate of the DCO's output is constant during one update period, and its sampled value equals (see Fig. 2(b))

$$\hat{\theta}_n = \hat{\theta}_0 + \sum_{j=1}^{n} \Delta\hat{\dot{\theta}}_j \quad (26)$$

The transfer function for a DCO is

$$\frac{\hat{\theta}(s)}{\hat{\dot{\theta}}(z)} = \frac{1 - e^{-sT_L}}{s^2} \quad (27a)$$

Our subcarrier demodulation loop has, in addition, a summer built on the DCO board. Taking this into account, the total "DCO board" transfer function becomes

$$\frac{\theta(s)}{\Delta\hat{\dot{\theta}}(z)} = \left(\frac{1 - e^{-sT_L}}{s^2}\right)\frac{z}{z - 1} \quad (27b)$$

IV. Phase Detector Averages

The phase rate error process $\phi(t)$ is shown in Fig. 2(a). At frequency update instants, it is expressed by the following difference equation

$$\dot{\phi}_n = \dot{\phi}_{n-1} + T_L \ddot{\phi}_{n-1} - \Delta\hat{\dot{\theta}}_n \tag{28}$$

with

$$T_L = T_R + T_c \tag{29}$$

where

T_L = the frequency update period in seconds, and

$T_c = T_L g$, the computation time, in seconds, with

$$0 \leqslant g < 1. \tag{30}$$

The phase error process $\phi(t)$ at frequency update instants is obtained by integrating $\phi(t)$ between t_{n-1} and t_n, namely

$$\phi_n = \phi_{n-1} + \dot{\phi}_{n-1} T_L + \ddot{\phi}_{n-1} \frac{T_L^2}{2} \tag{31}$$

Referring to Fig. 2, we want to find the integrated phase error over one update period

$$\bar{\phi}_n = \left[\int_{t_n - T_c}^{t_n} \phi(t)\, dt + \int_{t_n}^{t_n + T_R} \phi(t)\, dt \right] \tag{32}$$

The algebra in finding $\bar{\phi}_n$ is straightforward but a little lengthy.

It can be shown that

$$\bar{\phi}_n = T_L \left(\phi_n + \frac{1}{2} T_L (1 - 2g) \dot{\phi}_n + \frac{1}{6} T_L^2 (1 - 3g + 3g^2) \ddot{\phi}_n - \frac{T_L}{2} g^2 \Delta\dot{\theta}_n \right) \tag{33}$$

where the normalized computation time g is defined by (30).

Using (33) together with (4), the normalized average phase error corresponding to Eq. (6) is

$$u_n = \frac{2}{\pi T_L} \bar{\phi}_n$$

$$= \left(\frac{2}{\pi T_L} \right) T_L \times \left[1 \quad \frac{T_L}{2}(1 - 2g) \quad \frac{T_L^2}{6}(1 - 3g + 3g^2) \quad - \frac{T_L}{2} g^2 \right] \begin{bmatrix} \phi_n \\ \dot{\phi}_n \\ \ddot{\phi}_n \\ \Delta\hat{\dot{\theta}}_n \end{bmatrix} \tag{34}$$

or

$$u_n = \left(\frac{2}{\pi T_L} \right) \bar{T}' \cdot \bar{\Phi}_n \tag{35}$$

where $\bar{T}'$ is the row vector of (34) including the multiplication by T_L, and $\bar{\Phi}_n$ is the rightmost column vector.

V. Closed Loop Transfer Function

Combining Eqs. (21), (32) and (35), we get

$$\bar{\epsilon}_n = G'_Q \frac{2}{T_L \pi} \int_{t_n - T_c}^{t_n + T_R} \phi(t)\, dt \tag{36}$$

$$= G'_Q \frac{2}{T_L \pi} \bar{T}' \cdot \bar{\phi}_n \tag{37}$$

The z-transform of the output C_n of an integrate-and-dump device with gain G and continuous input $R(t)$ is, according to Ref. 2,

$$C(z) = G \frac{z - 1}{z} \left(\frac{R(s)}{s} \right)^* \tag{38}$$

where $R(s)$ is the Laplace transform of $R(t)$ and the asterisk denotes a z-transform. Letting

$$G_Q = G'_Q \frac{2}{T_L \pi} = \frac{K K_1 K_2 K_3 N_s^2 S}{T_L \pi} \tag{39}$$

then from (37) and (38), we obtain

$$\bar{\epsilon}(z) = G_Q \frac{z - 1}{z} \left(\frac{\Phi(s)}{s} \right)^* \tag{40}$$

where $\Phi(s)$ is the Laplace transform of $\phi(t)$.

The time delay between the instants in which the error signal ϵ_n is read and the phase rate update $\Delta\theta_n$ is produced, is modelled as

$$D(s) = e^{-g T_L s} \tag{41}$$

Equations (25), (27), (40) and (41) now can be combined to give the block diagram of Fig. 3, which is a hybrid Laplace z-transform equivalent representation of the subcarrier demodulation loop.

Referring to Fig. 3,

$$X(s) = \frac{\phi(s)}{s} = \frac{\theta(s)}{s} - \Delta\hat{\theta}(z)\frac{e^{-gT_L s}}{s^3}(1 - e^{-sT_L})\frac{z}{z-1} \tag{42}$$

$$= \frac{\theta(s)}{s} - \Delta\hat{\theta}(z)\frac{e^{-gT_L s}}{s^3} \tag{43}$$

because $e^{-sT_L} \triangleq z^{-1}$.

Taking the z-transform on both sides of (43),

$$X(z) = \left(\frac{\phi(s)}{s}\right)^* = \left(\frac{\theta(s)}{s}\right)^* - \Delta\hat{\theta}(z)\left(\frac{e^{-gT_L s}}{s^3}\right)^* \tag{44}$$

In general, given a function $L(s)$, we always have

$$[e^{-\delta Ts}L(s)]^* = L(z, m), \qquad m = 1 - g \tag{45}$$

where $L(z, m)$ is the modified z-transform of $L(s)$.

Using this property in (44),

$$X(z) = \left(\frac{\theta(s)}{s}\right)^* - \frac{T_L^2[m^2z^2 + (2m - 2m^2 + 1)z + (m-1)^2]}{2(z-1)^3}\Delta\hat{\theta}(z) \tag{46}$$

or

$$= \left(\frac{\theta(s)}{s}\right)^* - \frac{T_L^2[(1-g)^2z^2 + (1 + 2g - 2g^2)z + g^2]}{2(z-1)^3}\Delta\hat{\theta}(z) \tag{47}$$

Combining Eqs. (25), (40) and (47), the block diagram shown in Fig. 4 is obtained.

The open loop transfer function corresponding to Fig. 4 is

$$G(z) = \frac{\hat{\theta}_1(z)}{X(z)}$$

$$= G\frac{((1-g)^2z^2 + (1 + 2g - 2g^2)z + g^2)(zA + B)}{(z-1)^2(z^2 - zC - D)} \tag{48}$$

where

$$G = \frac{T_L^2}{2}G_Q \tag{49}$$

The closed loop transfer function is

$$H(z) = \frac{\hat{\theta}_1(z)}{\theta_1(z)} = \frac{G(z)}{1 + G(z)} \tag{50}$$

$$H(z) = \frac{G((1-g)^2z^2 + (1 + 2g - 2g^2)z + g^2)(zA + B)}{z^4 + z^3(GA(1-g)^2 - C - 2) + z^2(1 + 2C - D \cdots + GA(1 + 2g - 2g^2) + GB(1-g)^2 \cdots + z(2D - C + GAg^2 + GB(1 + 2g - 2g^2)) - D + GBg^2} \tag{51}$$

The denominator of (51) is designated as the characteristic polynomial of the loop, which we define as $C(z)$.

VI. Determination of Gains *A*, *B*, *C* and *D*

For stability, we want the poles of $H(z)$ to be inside the unit circle. To avoid instability and oscillation problems when the gain G changes slightly for whatever reasons, we choose to place all four poles on the real axis such that

$$p_1 = p_2 = \text{small negative number}$$

and (52)

$$p_3 = p_4 \text{ between 0.3 and 0.7.}$$

As such, poles p_3 and p_4 will determine the transient response of the closed loop. Using (52), let

$$C(z) = (z - p_1)^2(z - p_3)^2$$

$$= z^4 + 2(-p_1 - p_3)z^3 + (p_3^2 + 4p_1p_3 + p_1^2)z^2 + 2(-p_1p_3^2 - p_1^2p_3^2)z + p_1^2p_3^2 \tag{53}$$

Equating the coefficients of equal powers in the polynomials of Eq. (53) and the denominator of (51), we obtain four equations with four unknowns which can be written in the following matrix form

$$\begin{bmatrix} G(1-g)^2 & 0 & -1 & 0 \\ G(1+2g-2g^2) & G(1-g)^2 & 2 & -1 \\ Gg^2 & G(1+2g-2g^2) & -1 & 2 \\ 0 & Gg^2 & 0 & -1 \end{bmatrix} \begin{bmatrix} A \\ B \\ C \\ D \end{bmatrix} = \begin{bmatrix} a_3+2 \\ a_2-1 \\ a_1 \\ a_0 \end{bmatrix} \tag{54}$$

where, from (53), we have

$$\begin{aligned} a_0 &= p_1^2 p_3^2 \\ a_1 &= -2(p_1 p_3^2 + p_1^2 p_3) \\ a_2 &= p_3^2 + 4p_1 p_3 + p_1^2 \\ a_3 &= -2(p_1 + p_3) \end{aligned} \tag{55}$$

Table 1 gives values for the gains A, B, C and D when $G = 1.0$, $p_1 = -0.1$, $p_3 = 0.6$ and $g = 0$, 0.25 and 0.5.

The root locus diagrams for $g = 0$ and $g = 0.5$ for G changing between 0 (open loop) to 2 (unstable loop) are shown in Fig. 5. As we see from this figure, when nominal total loop gains GA, GB are selected, two pairs of poles at -0.1 and two pairs of poles at 0.6 are obtained. In both cases ($g = 0$ and $g = 0.5$) the loop will lock without oscillations. The settling time, t_s, will be determined by p_3 and p_4 and will be, in our case,

$$t_s \cong \frac{4T_L}{-\ln p_3} = 7.8 \text{ seconds} \tag{56}$$

if $T_L = 1$ second.

The Nyquist plot corresponding to the selected nominal gains for $g = 0$ is shown in Fig. 6 and the Bode diagram in Fig. 7. For nominal loop gain, the

$$\text{Gain margin} = -20 \log_{10} |G(z)| \Big|_{\underline{/G(z)} = 180^\circ} \cong 10 \text{ dB} \tag{57}$$

and

$$\text{Phase margin} = 180 - \underline{/G(z)} \Big|_{|G(z)| = 0 \text{ dB}} \cong 50 \text{ deg} \tag{58}$$

To doublecheck the stability of our loop, let

$$C'(z) = a_4 z^4 + a_3 z^3 + a_2 z^2 + a_1 z + a_0 \tag{59}$$

be the polynominal of the denominator of the closed loop transfer function $H(z)$ given by (51). The Jury stability test (Ref. 3) requires that the following conditions be met:

$$\begin{aligned} &(1)\ C'(1) > 0 \\ &(2)\ C'(-1) > 0 \\ &(3)\ |a_0| < a_4 = 1 \\ &(4)\ |b_0| > |b_3| \\ &(5)\ |C_0| > |C_2| \end{aligned} \tag{60}$$

where

$$\begin{aligned} b_k &= \begin{vmatrix} a_0 & a_{4-k} \\ a_4 & a_k \end{vmatrix} \\ C_k &= \begin{vmatrix} b_0 & b_{3-k} \\ b_3 & b_k \end{vmatrix} \end{aligned} \tag{61}$$

Using the nominal gain values of Table 1 to compute a_0, a_1, a_2, a_3, and a_4, it is straightforward to show that these conditions are met.

VII. Steady State Error

For a parabolic input

$$\theta(t) = \ddot{\theta}_p t^2, \tag{62}$$

the z-transform of the equivalent input in Fig. 4 is

$$\theta_1(z) = \left(\frac{\theta(s)}{s}\right)^* = \frac{\ddot{\theta}_p T_L^3 z(z^2 + 4z + 1)}{6(z-1)^4} \tag{63}$$

Our transfer function now is defined as

$$H_\epsilon(z) = \frac{\epsilon(z)}{\theta_1(z)} \tag{64}$$

From Fig. 4, $H_\epsilon(z)$ is

$$H_\epsilon(z) = \frac{z-1}{z} \times \frac{G_Q}{1 + \dfrac{G((1-g)^2z^2 + (1+2g-2g^2)z + g^2)(zA+B)}{(z-1)^2(z^2 - zC - D)}} \tag{65}$$

The steady state error is defined as

$$\bar{\epsilon}_{ss} = \lim_{n\to\infty} \bar{\epsilon}_n = \lim_{z\to 1}\left(\frac{z-1}{z}\right) H_\epsilon(z)\,\theta_1(z) \tag{66}$$

Inserting (63) and (65) into (66) and letting z go to one, the steady state error signal at sampling instants due to a parabolic input is

$$\bar{\epsilon}_{ss} = \frac{\ddot{\theta}_p T_L (1 - C - D)}{(A+B)} \tag{67}$$

Equation (67) says that our subcarrier demodulation loop can track a parabolic input with a finite steady state error which is independent of the normalized computation time, g.

VIII. Derivation of the State and Output Equations

Using (33) in (37), the error signal evaluated at sample time $n-1$ is

$$\epsilon_{n-1} = G_Q\left(T_L\phi_{n-1} + \frac{1}{2}T_L{}^2(1-2g)\dot{\phi}_{n-1} + \frac{1}{2}T_L{}^3\left(\frac{1}{3} - g + g^2\right)\ddot{\phi}_n - \frac{T_L{}^2}{2}g^2\,\Delta\hat{\theta}_{n-1}\right) + \eta_{n-1} \tag{68}$$

The error signal at time $n-2$ can be expressed in terms of its value at time $n-1$, namely,

$$\epsilon_{n-2} = G_Q\left(T_L\phi_{n-1} - \frac{1}{2}T_L{}^2(1+2g)\dot{\phi}_{n-1} + \frac{T_L{}^3}{2}\left(\frac{1}{3} + g + g^2\right)\ddot{\phi}_n - \frac{T_L{}^2}{2}(1+2g)\,\Delta\hat{\theta}_{n-1} - \frac{T_L{}^2}{2}g^2\,\Delta\hat{\theta}_{n-2}\right) + \eta_{n-2} \tag{69}$$

Inserting (68) and (69) into (23) and combining terms gives

$$\Delta\hat{\theta}_n = G_Q T_L(A+B)\phi_{n-1} + \frac{G_Q T_L{}^2}{2}[A(1-2g) - B(1+2g)]\dot{\phi}_{n-1} + \frac{T_3{}^3}{2}G_Q\left[A\left(\frac{1}{3} - g + g^2\right) - B\left(\frac{1}{3} + g + g^2\right)\right]\ddot{\phi}_n + \left[C - G_Q\frac{T_L{}^2}{2}(Ag^2 + B(1+2g))\right]\Delta\hat{\theta}_{n-1} + \left(D - \frac{G_Q}{2}T_L{}^2g^2B\right)\Delta\hat{\theta}_{n-2} + A\eta_{n-1} + B\eta_{n-2} \tag{70}$$

Let

$$X = G_Q T_L(A+B)$$

$$V = G_Q\frac{T_L{}^2}{2}[A(1-2g) - B(1+2g)]$$

$$Y = C - G_Q\frac{T_L{}^2}{2}[Ag^2 + B(1+2g)]$$

$$W = \frac{T_L{}^3}{2}G_Q\left[A\left(\frac{1}{3} - g + g^2\right) - B\left(\frac{1}{3} + g + g^2\right)\right]$$

$$U = D - \frac{G_Q T_L{}^2}{2}g^2B \tag{71}$$

Then, Eq. (70) can be rewritten as

$$\Delta\hat{\dot{\theta}}_n = X\phi_{n-1} + V\dot{\phi}_{n-1} + W\ddot{\phi}_{n-1} + Y\Delta\hat{\dot{\theta}}_{n-1} + U\Delta\hat{\dot{\theta}}_{n-2} + A\eta_{n-1} + B\eta_{n-2} \quad (72)$$

Referring to Fig. 3, we have

$$x_2(k+1) = x_1(k)$$

or

$$\Delta\hat{\dot{\theta}}_{n-2+1} = \Delta\hat{\dot{\theta}}_{n-1} \quad (73)$$

Inserting (72) into (28) gives

$$\dot{\phi}_n = -X\phi_{n-1} - Y\Delta\hat{\dot{\theta}}_{n-1} - U\Delta\hat{\dot{\theta}}_{n-2} + (1-V)\dot{\phi}_{n-1} + (T_L - W)\ddot{\phi}_{n-1} - A\eta_{n-1} - B\eta_{n-2} \quad (74)$$

Combining Eqs. (31), (74), (72) and (73) in matrix form, we obtain the State Equation:

$$\begin{pmatrix} \phi_n \\ \dot{\phi}_n \\ \Delta\hat{\dot{\theta}}_n \\ \Delta\hat{\dot{\theta}}_{n-1} \end{pmatrix} = \begin{pmatrix} 1 & T_L & 0 & 0 \\ -X & 1-V & -Y & -U \\ X & V & Y & U \\ 0 & 0 & 1 & 0 \end{pmatrix} \begin{pmatrix} \phi_{n-1} \\ \dot{\phi}_{n-1} \\ \Delta\hat{\dot{\theta}}_{n-1} \\ \Delta\hat{\dot{\theta}}_{n-2} \end{pmatrix} + \begin{pmatrix} T_L^2/2 & 0 & 0 & 0 \\ T_L - W & -A & -B & 0 \\ W & A & B & 0 \\ 0 & 0 & 0 & 0 \end{pmatrix} \begin{pmatrix} \ddot{\phi}_{n-1} \\ \eta_{n-1} \\ \eta_{n-2} \\ 0 \end{pmatrix} \quad (75)$$

which is of the form

$$x(k+1) = \mathcal{A}x(k) + \mathcal{B}u(k) \quad (76)$$

The Output Equation is (rewriting (68) in vector form):

$$\epsilon_n = G_Q \begin{pmatrix} T_L & \frac{1}{2}T_L^2(1-2g) & -\frac{T_L^2}{2}g & 0 \end{pmatrix} \begin{pmatrix} \phi_n \\ \dot{\phi}_n \\ \Delta\hat{\dot{\theta}}_n \\ \Delta\hat{\dot{\theta}}_{n-1} \end{pmatrix} + \begin{pmatrix} G_Q & \frac{T_L^3}{2}\left(\frac{1}{3} - g + g^2\right) & 1 & 0 & 0 \end{pmatrix} \begin{pmatrix} \ddot{\phi}_n \\ \eta_n \\ \eta_{n-1} \\ 0 \end{pmatrix} \quad (77)$$

which is of the form

$$\epsilon(k) = \bar{\mathcal{D}}x(k) + \bar{\mathcal{E}}u(k) \quad (78)$$

The characteristics polynomial $C(z)$ is

$$C(z) = \det(zI - \mathcal{A}) \quad (79)$$

where $\mathcal{A}$ is the matrix defined in (76). Inserting $\mathcal{A}$ into (79), we obtain

$$C(z) = \det \begin{bmatrix} z-1 & -T_L & 0 & 0 \\ X & z-V-1 & Y & U \\ -X & -V & z-Y & -U \\ 0 & 0 & -1 & z \end{bmatrix}$$

$$= z^4 + z^3(V - Y - 2) + z^2(2Y - V - U + 1 + T_L X) + z(2U - Y) - U \quad (80)$$

Using the definitions of (71), we obtain

$$C(z) = z^4 + [GA(1-g)^2 - 2 - C]z^3 + [2C - D + 1 + GA(1 + 2g - 2g^2) + GB(1-g)^2]z^2 + [2D - C + GAg^2 + GB(1 + 2g - 2g^2)]z - D + GBg^2 \quad (81)$$

Comparing (81) to the denominator of $H(z)$ in Eq. (51), we see that both polynomials are identical, as they should be.

The state equation given by (75) will be needed to derive the steady state values of $\phi, \dot{\phi}$ and $\Delta\dot{\theta}$.

IX. Noise-Equivalent Bandwidth

Referring to Fig. 4, the closed loop transfer function $H(z)$ is given by Eq. (51). The one-sided noise-equivalent bandwidth is defined as

$$B_L = \frac{1}{2T_L}\,\frac{1}{H^2(1)}\,\frac{1}{2\pi j}\oint H(z)\,H(z^{-1})\frac{dz}{z} \tag{82}$$

It can be shown that

$$H^2(1) \equiv 1 \tag{83}$$

for all values of A, B, C, D, g and G.

To evaluate (82), we express $H(z)$ of (51) as a ratio of polynomials,

$$H(z) = \frac{b_0 z^4 + b_1 z^3 + b_2 z^2 + b_3 z + b_4}{a_0 z^4 + a_1 z^3 + a_2 z^2 + a_3 z + a_4} \tag{84}$$

and then make use of the results in Table III.4 of Ref. 3.

If we define

$$I_4 = \frac{1}{2\pi j}\oint H(z)\,H(z^{-1})\frac{dz}{z} \tag{85}$$

then, from Ref. 4 we have

$$I_4 = \frac{a_0 B_0 Q_0 - a_0 B_1 Q_1 + a_0 B_2 Q_2 - a_0 B_3 Q_3 + B_4 Q_4}{a_0\left[(a_0^2 - a_4^2)\,Q_0 - (a_0 a_1 - a_3 a_4)\,Q_1 + (a_0 a_2 - a_2 a_4)\,Q_2 - (a_0 a_3 - a_1 a_4)\,Q_3\right]} \cdots \tag{86}$$

where

$$B_0 = b_0^2 + b_1^2 + b_2^2 + b_3^3 + b_4^2$$

$$B_1 = 2(b_0 b_1 + b_1 b_2 + b_2 b_3 + b_3 b_4)$$

$$B_2 = 2(b_0 b_2 + b_1 b_3 + b_2 b_4)$$

$$B_3 = 2(b_0 b_3 + b_1 b_4)$$

$$B_4 = 2 b_0 b_4$$

$$Q_0 = a_0 e_1 e_4 - a_0 a_3 e_2 + a_4(a_1 e_2 - e_3 e_4)$$

$$Q_1 = a_0 a_1 e_4 - a_0 a_2 a_3 + a_4(a_1 a_2 - a_3 e_4)$$

$$Q_2 = a_0 a_1 e_2 - a_0 a_2 e_1 + a_4(a_2 e_3 - a_3 e_2)$$

$$Q_3 = a_1(a_1 e_2 - e_3 e_4) - a_2(a_1 e_1 - a_3 e_3) + a_3(e_1 e_4 - a_3 e_2)$$

$$Q_4 = a_0[e_2(a_1 a_4 - a_0 a_3) + e_5(a_0^2 - a_4^2)] + (e_2^2 - e_5^2)\,[a_1(a_1 - a_3) + (a_0 - a_4)(e_4 - a_2)]$$

$$e_1 = a_0 + a_2$$

$$e_2 = a_1 + a_3$$

$$e_3 = a_2 + a_4$$

$$e_4 = a_0 + a_4$$

$$e_5 = a_0 + a_2 + a_4 \tag{87}$$

Using the above results, the one-sided noise-equivalent bandwidths for given values of g, A, B, C, D and G are listed in Table 2.

X. Conclusion

The BBA's subcarrier demodulation digital loop, a fourth-order Costas-type loop, has been analyzed in this article. The mean value and variance of the error signal have been found. A block diagram in the z-domain has been obtained from which optimum gains of the loop filter have been found. These gains will keep the four poles of the transfer function on the real axis inside the unit circle. The loop is able to track a parabolic input with finite steady state error, as it is a type-2 analog loop. One-sided noise-equivalent bandwidths for given values of normalized computation time and gain values have been given.

References

1. "DSN/Flight Project Interface Design Handbook," JPL 810-5, Rev. D, Volume II, Module TLM-10, p. 4.

2. Winkelstein, R. A., "Analysis of the Signal Combiner for Multiple Antenna Arraying," Deep Space Network Progress Report 42-26, January and February 1975, pp. 102-118.

3. Jury, E. I., "Theory and Applications of the Z-Transform Method," R. E. Krieger Publishing Co., Malabar, Florida, 1982.

Table 1. Loop gains for given pole locations[a]

Filter Gains	Computation Time Factor		
	$g = 0.0$	$g = 0.25$	$g = 0.5$
A	0.5248	0.5390	0.5632
B	-0.4180	-0.4422	-0.4664
C	-0.4852	-0.6968	-0.8592
D	-0.0036	-0.0312	-0.1202

[a] $p_1 = p_2 = -0.1$. $p_3 = p_4 = 0.6$. $G = 1.0$.

Table 2. Noise-equivalent one-sided bandwidth in Hz for gains *A*, *B*, *C* and *D* given in Table 1

Gain G	Computation Time Factor		
	$g = 0.0$	$g = 0.25$	$g = 0.5$
1.0	0.3324	0.3858	0.4395
0.5	0.1696	0.1744	0.1814
0.1	0.0792	0.0768	0.0748
0.01	0.0620	0.0604	0.0589
0.001	0.0603	0.0588	0.0573

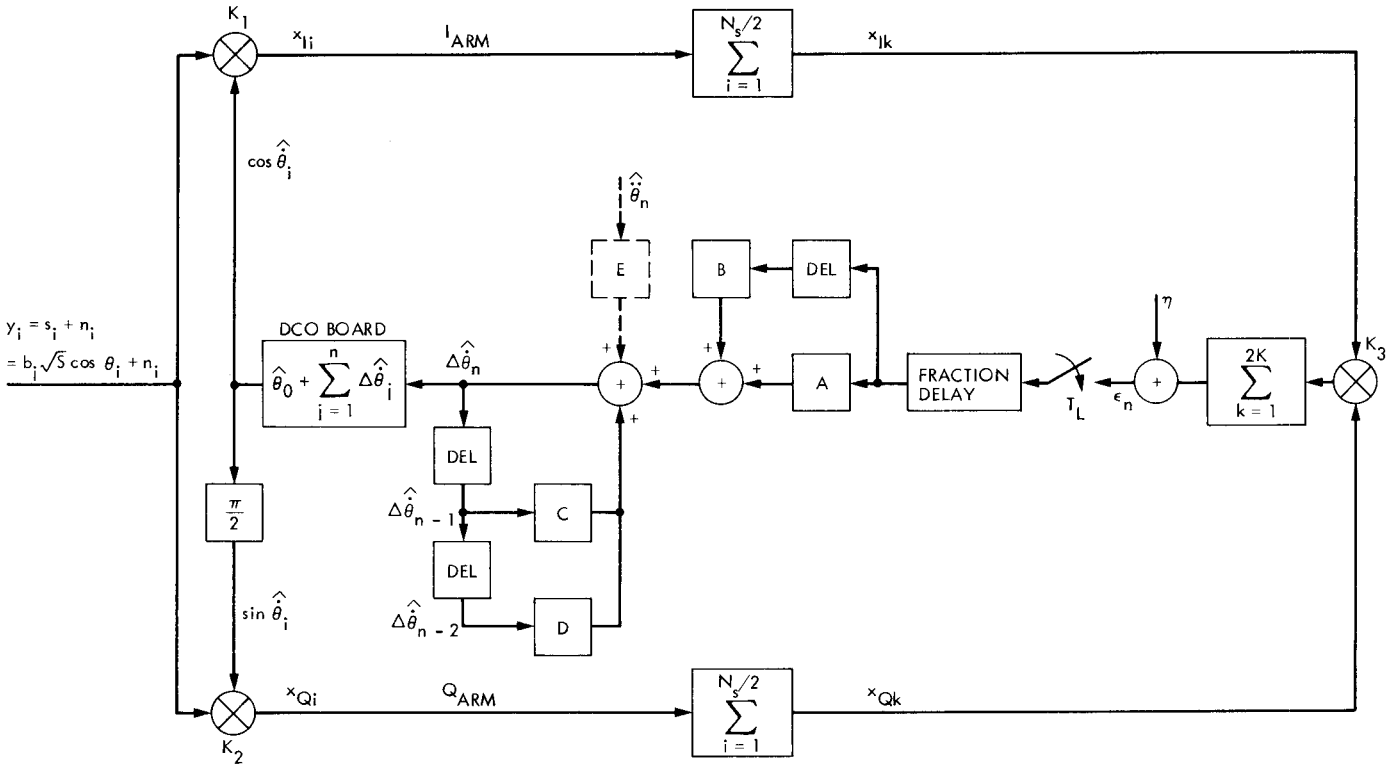

Fig. 1. Subcarrier demodulation loop

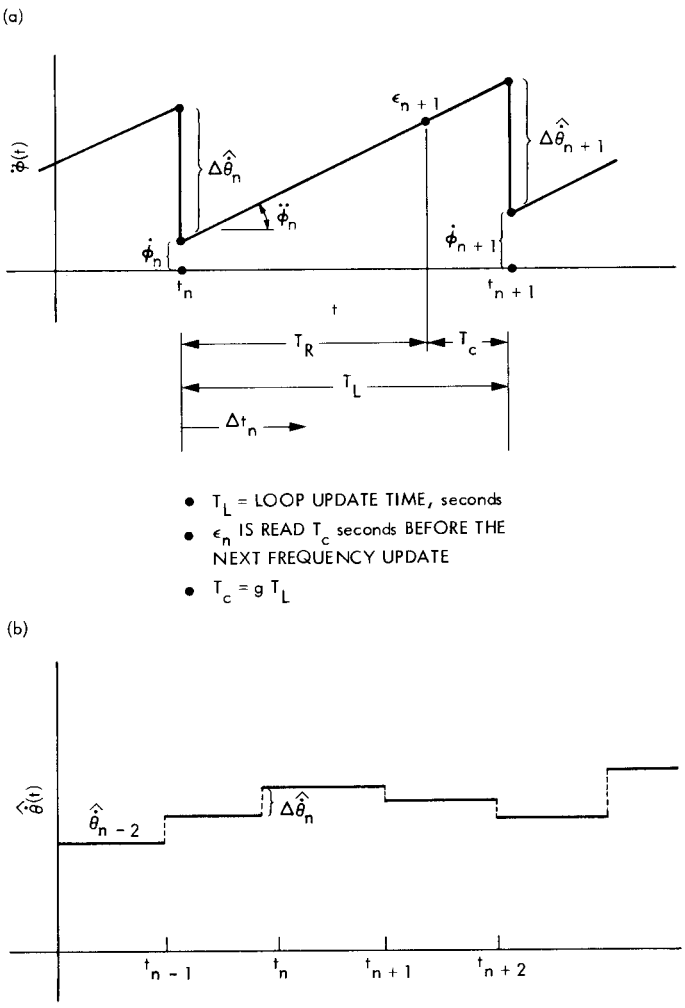

Fig. 2. Phase rate (a) error, and (b) DCO output

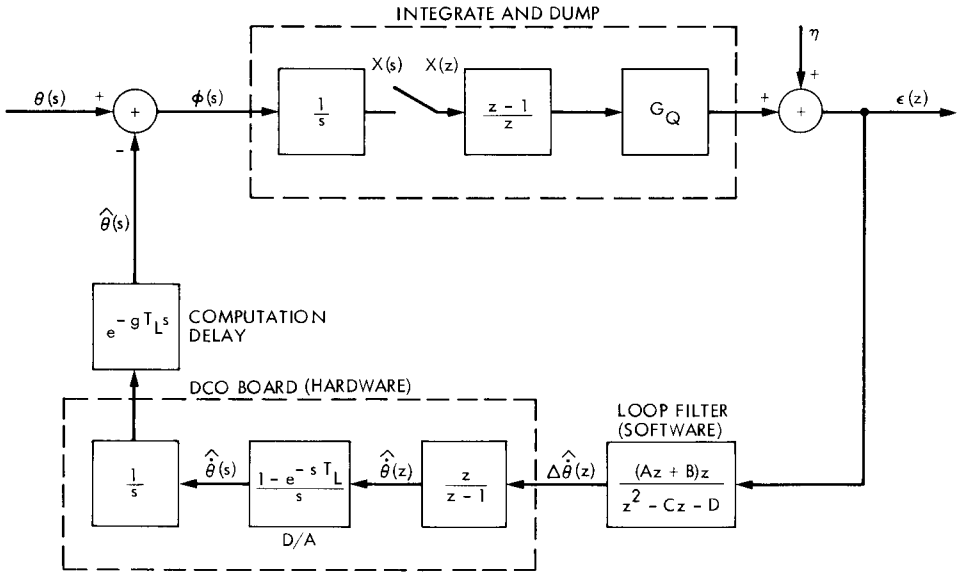

Fig. 3. Closed loop hybrid s/z diagram. Note that a conventional DCO does not include the z/(z − 1) transfer function as shown here as an integral part of the DCO board.

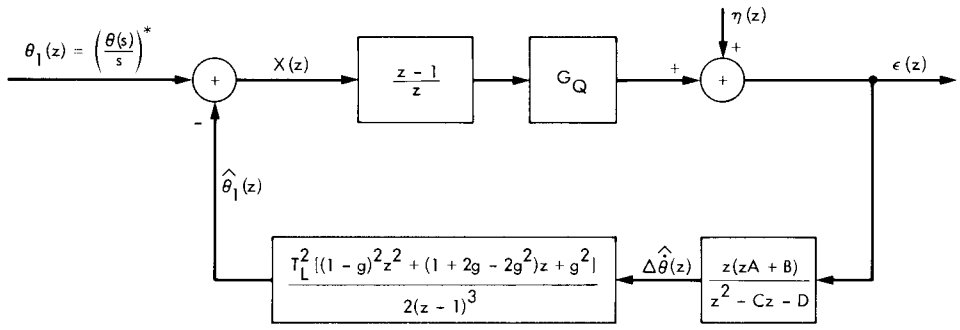

Fig. 4. Equivalent z-domain block diagram

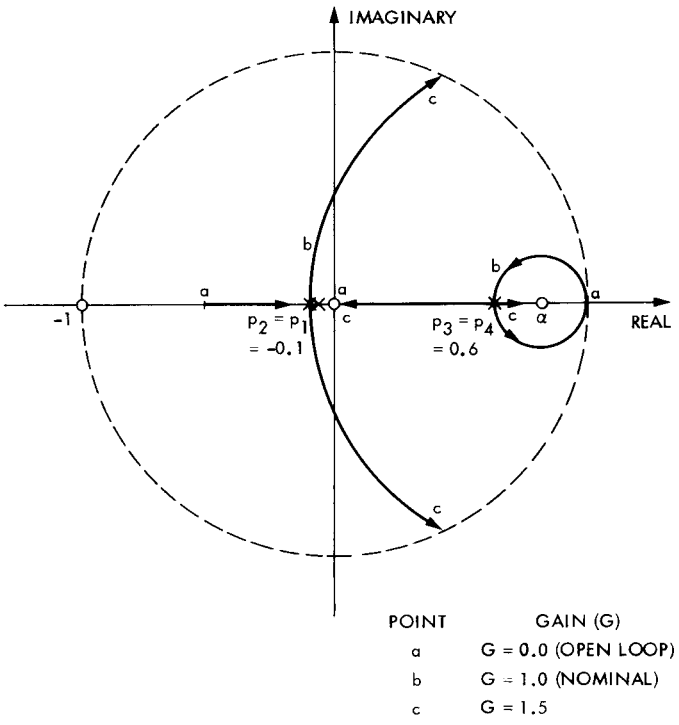

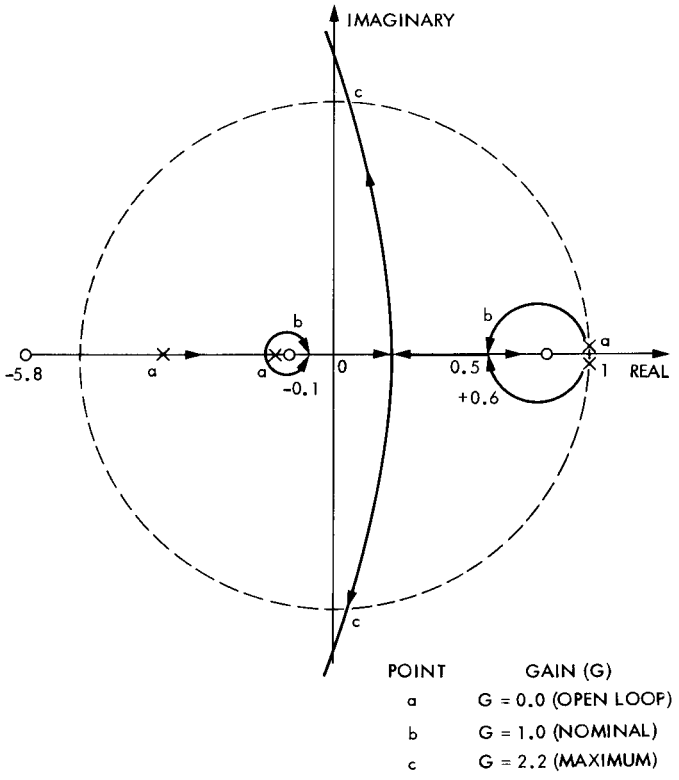

Fig. 5. Root locus diagram for (a) g = 0.0, and (b) g = 0.5

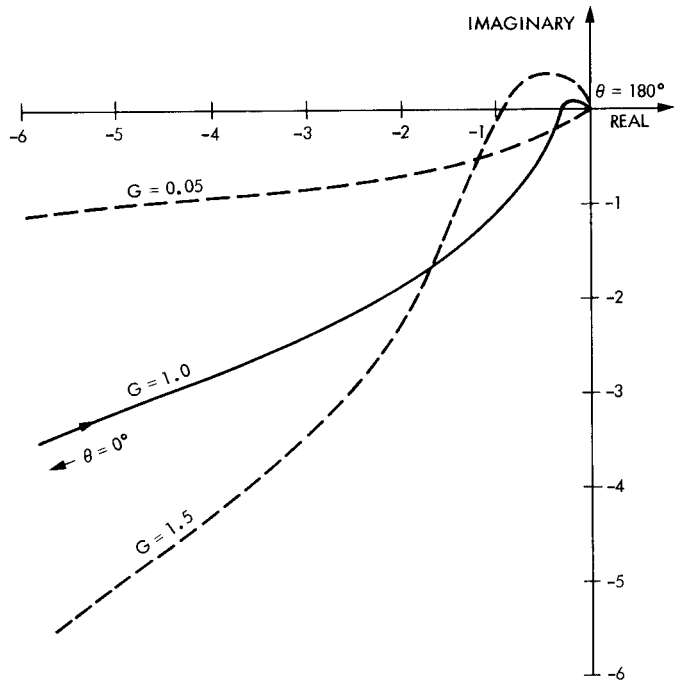

Fig. 6. Frequency response loci of G(z) for a sample frequency of $\omega_s = 2/T_L$ and g = 0.0

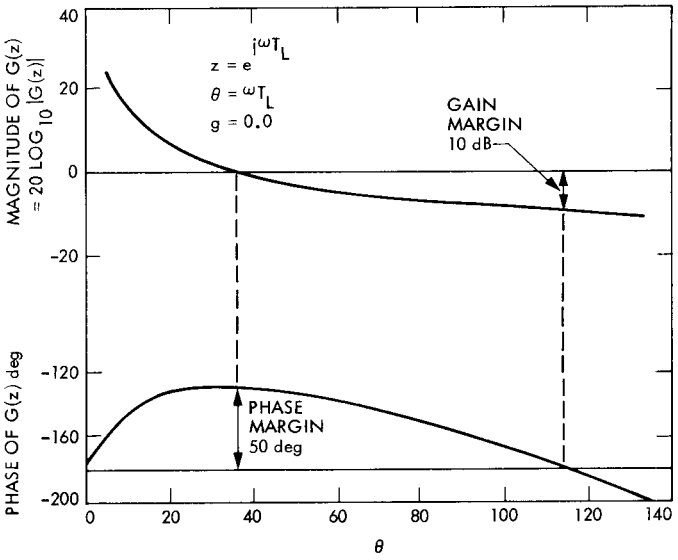

Fig. 7. Bode diagram of G(z) for nominal gains